Simulative analyse of turbine trains under blade fracture conditions with regard to the implementation methods of journal bearings

E. Woschke, C. Daniel, S. Nitzschke
Otto-von-Guericke-University Magdeburg, Faculty of Mechanical Engineering, Institute of Mechanics (Fluid Structure Interaction & Technical Dynamics), Germany

ABSTRACT
Concerning the design of rotor systems supported by journal bearings, worst-case scenarios represent a highly sensitive investigation. Beside the actual rotor dynamic parameters, especially the nonlinear bearing characteristics have a significant influence on the behaviour of the system and the resulting risk potential. The paper gives an overview on the possibilities of numerical analysis of rotor systems with journal bearings under dynamic conditions. Simulation results for a turbine train excited by a sudden blade fracture are analysed using different modelling approaches concerning the bearings in context of reliability and simulation time.

1 INTRODUCTION

Due to the high effort of experimental investigations concerning dynamical load cases, simulations are increasingly used. Depending on the actual application transient system behaviour refers to run-up or run-down situations, worst-case scenarios or even typical operating conditions.
In conventional rotordynamic simulations the nonlinear behaviour of the journal bearings is often implemented using significant simplifications. Although the basic differential equation for the description of the hydrodynamic effects are known, a holistic solution is numerical costly especially in context of time integration schemes. As a result, often lookup tables are used ignoring the effects of misalignments or even analytical formulations like short bearing theory without the possibility to consider boundary conditions for oil supply.
On the other hand, for simulations with focus on the hydrodynamic bearings the rotor is often oversimplified to a mass point and the mechanical system behaviour is modelled under steady-state conditions whereas the hydrodynamic equations are solved with high modelling depth.
Especially for critical system conditions a reliable calculation of vibration amplitudes, acting forces, minimal gaps etc. is crucial. At that point, advanced simulations with both a detailed description of the hydrodynamics and an adequate modelling of the rotordynamic behaviour are necessary.

2 MODEL OF THE TURBINE TRAIN

The turbine train to be investigated has a length of $l = 68\,m$ and 278 shaft shoulders varying in diameter from $d_{min} = 450\,mm$ to $d_{max} = 1600\,mm$. The turbine wheels are modelled as rigid bodies with a mean diameter to achieve an adequate rotor model by means of dominant stiffness and mass properties. A detailed description of the wheel-blades and their interaction is neither the focus of the paper nor relevant for rotordynamic analyses.

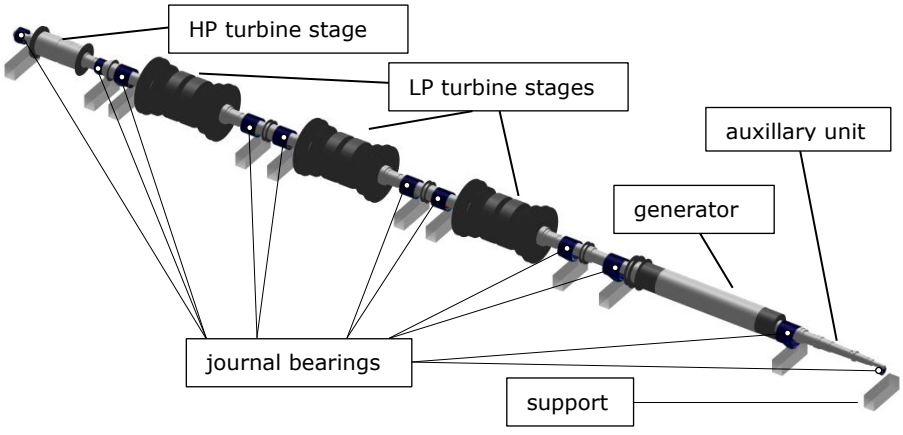

Figure 1 - Modell of the turbine train including 11 journal bearings

The rotor is supported in 11 journal bearings. The acting forces are determined by gravity, leading to a static deformation of the shaft, and by unbalance at the turbine wheels as well as on the generator. For general use, the rotor system will run under steady-state conditions at a rotational speed of $\Omega = 2\pi\ 25Hz = const.$

Beside linear investigations (e.g. eigenvalue calculation and harmonic analysis), due to the behaviour of journal bearings, nonlinear rotordynamic simulations are necessary, whereas the majority of computational methods is limited to the described load case, with varying modelling depth concerning the hydrodynamics. In case of dynamic conditions like due to a critical fault (e.g. blade fracture) the investigation of the rotor system becomes more sophisticated. For that task, a holistic model including a direct interaction between rotordynamic and hydrodynamic is needed.

3 ROTORDYNAMIC - EQUATIONS OF MOTION

The elastic properties of the turbine train are determined by the geometric dimensions and the assigned material of the rotor. The assembly performs small motions, except the rotation around the longitudinal axis. Therefore, under the restriction of circular cross sections, the overall-motion can be described by means of a linear finite element model. Also - beside the stiffness property - inertia and damping effects have to be taken into account to be able to handle transient effects.

3.1 Finite beam element

As the main dimension of the shaft is determined by its length, considering the existence of short shoulders, a beam model based on the Timoshenko-theory is appropriate.

Following the approach for rotating structures given in (1), the equation of motions becomes

$$\underline{\underline{M}}\,\ddot{\underline{x}} + \left(\underline{\underline{D}} + \Omega\,\underline{\underline{G}}\right)\,\dot{\underline{x}} + \underline{\underline{K}}\,\underline{x} = \underline{f} \quad , \qquad \text{Eq. 1}$$

where $\underline{\underline{M}}$ denotes the mass matrix, $\underline{\underline{K}}$ the stiffness matrix and $\underline{\underline{G}}$ the skew-symmetric gyroscopic matrix. Finally, the damping of the structure is considered by the Rayleigh approach $\underline{\underline{D}} = \alpha\,\underline{\underline{M}} + \beta\,\underline{\underline{K}}$.

The vector $\underline{f}$ on the right-hand-side contains the distributed load due to gravity, the unbalance induced forces and the reaction forces of the bearings, which are described detailed in chapter 4.

Starting from some initial conditions for positions $\underline{x}$ as well as for velocities $\underline{\dot{x}}$, Eq. 1 is solved for the current accelerations $\underline{\ddot{x}}$, which are integrated numerically. Due to the coupled hydro-structural dynamic task, a semi-implicit integration scheme, which is capable to deal with stiff problems, is necessary.
The investigated turbine train consists of a variety of shaft shoulders, which presupposes a fine discretisation and by that several degrees of freedom to ensure a realistic modelling. However, since only some nodes are excited by external loads or interact with the environment (nonlinear bearing forces), a system reduction is suitable to reduce the computation time.

3.2 Improved reduction system method

For structural-mechanical simulations based on finite element formulations system reduction is an effective way to reduce the numerical effort. Especially in the context of dynamic simulations including non-linear force laws, which leads to numerical stiff problems, the number of degrees of freedom has to be restricted due to demands of appropriate time integration methods.
Initially, a separation in master degrees of freedom $\{\}_{\mathbb{M}}$ (are still available after reduction and can be loaded by forces and moments) and slave-degrees of freedom $\{\}_{\mathbb{S}}$ (are no longer available after the reduction and has to be formally free of loads) takes place. The application on the equation of motion yields the following form

$$\begin{bmatrix} \underline{\underline{M}}_{\mathbb{MM}} & \underline{\underline{M}}_{\mathbb{MS}} \\ \underline{\underline{M}}^T_{\mathbb{MS}} & \underline{\underline{M}}_{\mathbb{SS}} \end{bmatrix} \begin{bmatrix} \underline{\ddot{x}}_{\mathbb{M}} \\ \underline{\ddot{x}}_{\mathbb{S}} \end{bmatrix} + \left(\begin{bmatrix} \underline{\underline{D}}_{\mathbb{MM}} & \underline{\underline{D}}_{\mathbb{MS}} \\ \underline{\underline{D}}^T_{\mathbb{MS}} & \underline{\underline{D}}_{\mathbb{SS}} \end{bmatrix} + \Omega \begin{bmatrix} \underline{\underline{G}}_{\mathbb{MM}} & \underline{\underline{G}}_{\mathbb{MS}} \\ \underline{\underline{G}}^T_{\mathbb{MS}} & \underline{\underline{G}}_{\mathbb{SS}} \end{bmatrix} \right) \begin{bmatrix} \underline{\dot{x}}_{\mathbb{M}} \\ \underline{\dot{x}}_{\mathbb{S}} \end{bmatrix} + \begin{bmatrix} \underline{\underline{K}}_{\mathbb{MM}} & \underline{\underline{K}}_{\mathbb{MS}} \\ \underline{\underline{K}}^T_{\mathbb{MS}} & \underline{\underline{K}}_{\mathbb{SS}} \end{bmatrix} \begin{bmatrix} \underline{x}_{\mathbb{M}} \\ \underline{x}_{\mathbb{S}} \end{bmatrix} = \begin{bmatrix} \underline{f}_{\mathbb{M}} \\ \underline{0} \end{bmatrix} \quad . \qquad \text{Eq. 2}$$

For the actual reduction a suitable transformation $\underline{\underline{Q}}_{red}$ has to be applied in order to describe the slave response as function of the master degrees of freedom

$$\begin{bmatrix} \underline{x}_{\mathbb{M}} \\ \underline{x}_{\mathbb{S}} \end{bmatrix} = \underline{\underline{Q}}_{red}\, \underline{x}_{\mathbb{M}} \quad . \qquad \text{Eq. 3}$$

Methods including a modal transformation (modal reduction, SEREP (2) etc.) are not suitable for the reduction of rotordynamic structures due the dependency of eigenvectors upon the angular velocity. However, there are different modal approaches but they are accompanied by a drastic numerical overhead and therefore are of a more academic nature (3).
For this reason, more conventional reduction methods have to be used. To avoid the known problems of static condensation (Guyan-reduction (4) - overestimation of stiffness) and component mode synthesis (CMS-reduction (5) - problematic choice of significant eigenmodes) a more generalised formulation called IRS-Method (Improved Reduction System Method) is applied (6).
In addition to the approach of Guyan given by

$$\begin{bmatrix} \underline{x}_{\mathbb{M}} \\ \underline{x}_{\mathbb{S}} \end{bmatrix} = \begin{bmatrix} \underline{\underline{I}} \\ -\underline{\underline{K}}^{-1}_{\mathbb{SS}}\, \underline{\underline{K}}^T_{\mathbb{MS}} \end{bmatrix} \underline{x}_{\mathbb{M}} = \underline{\underline{Q}}_G\, \underline{x}_{\mathbb{M}} \quad , \qquad \text{Eq. 4}$$

pseudo-static forces are taken into account as a result of inertia terms (6)

$$\underline{\underline{M}}_G\, \underline{\ddot{x}}_{\mathbb{M}} + \underline{\underline{K}}_G\, \underline{x}_{\mathbb{M}} = \underline{0} \qquad \Rightarrow \qquad \underline{\ddot{x}}_{\mathbb{M}} = -\underline{\underline{M}}^{-1}_G\, \underline{\underline{K}}_G\, \underline{x}_{\mathbb{M}} \quad . \qquad \text{Eq. 5}$$

With the time derivation of the transformation in Eq. 4 the acceleration of the slave-degrees of freedom can be formulated as

$$\underline{\ddot{x}}_{\mathbb{S}} = -\underline{\underline{K}}_{\mathbb{SS}}^{-1}\,\underline{\underline{K}}_{\mathbb{MS}}^{T}\,\underline{\underline{M}}_{G}^{-1}\,\underline{\underline{K}}_{G}\,\underline{x}_{\mathbb{M}} \quad . \qquad \text{Eq. 6}$$

Disregarding damping and gyroscopic terms, the equation of motion for the slave part can be written as

$$\underline{x}_{\mathbb{S}} = -\underline{\underline{K}}_{\mathbb{SS}}^{-1}\left(\underline{\underline{M}}_{\mathbb{MS}}^{T}\,\underline{\ddot{x}}_{\mathbb{M}} + \underline{\underline{M}}_{\mathbb{SS}}\,\underline{\ddot{x}}_{\mathbb{S}} + \underline{\underline{K}}_{\mathbb{MS}}^{T}\,\underline{x}_{\mathbb{M}}\right) \quad . \qquad \text{Eq. 7}$$

After a few rearrangements the transformation reads as

$$\begin{bmatrix}\underline{x}_{\mathbb{M}}\\ \underline{x}_{\mathbb{S}}\end{bmatrix} = \underline{\underline{Q}}_{IRS}\,\underline{x}_{\mathbb{M}} = (\underline{\underline{Q}}_{G} + \underline{\underline{P}}\,\underline{\underline{M}}\,\underline{\underline{Q}}_{G}\,\underline{\underline{M}}_{G}^{-1}\,\underline{\underline{K}}_{G})\,\underline{x}_{\mathbb{M}} \text{ with } \underline{\underline{P}} = \begin{bmatrix}\underline{\underline{0}} & \underline{\underline{0}}\\ \underline{\underline{0}} & \underline{\underline{K}}_{\mathbb{SS}}^{-1}\end{bmatrix} . \qquad \text{Eq. 8}$$

An improvement of the transformation can be gained by repeatedly executing the reduction. Though the stiffness and mass matrices of the static condensation have to be replaced by the resulting matrices of the previous IRS-step

$$\underline{\underline{Q}}_{IRS,i+1} = \underline{\underline{Q}}_{G} + \underline{\underline{P}}\,\underline{\underline{M}}\,\underline{\underline{Q}}_{IRS,i}\,\underline{\underline{M}}_{IRS,i}^{-1}\,\underline{\underline{K}}_{IRS,i} \quad , \qquad \text{Eq. 9}$$

where index i designates the i^{th} iteration. The algorithm converges monotonically with respect to the eigenvalues and eigenvectors of the unreduced system and by that is suitable for dynamic simulations.
In Figure 2 a comparison between the eigenfrequency dependence upon the rotational speed (Campbell-diagram) is presented for the examined turbine train under free-free boundary conditions. The results show an appropriate accordance between the dynamical behaviour of the reduced system (IRS) and the full model. Additionally, commonly used reduction methods (Guyan and CMS) are also included. As expected, the differences are higher w.r.t. the IRS reduction and increase with rotational speed. To ensure a better coincidence for Guyan and CMS, additional degrees of freedom has to be taken into account, whereas IRS method just needs more iteration steps without any necessity to increase system dimensions.

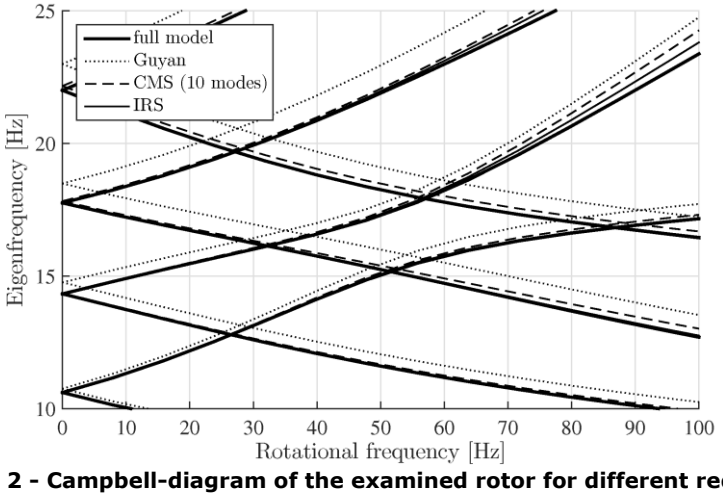

Figure 2 - Campbell-diagram of the examined rotor for different reduction methods

Finally, the reduced system matrices with $\underline{\underline{Q}}_{red} = \underline{\underline{Q}}_{IRS,conv}$ can be written as

$$\underline{\underline{S}}_{red} = \underline{\underline{Q}}_{red}^{T}\,\underline{\underline{S}}\,\underline{\underline{Q}}_{red} \qquad \text{with} \qquad \underline{\underline{S}} = \underline{\underline{M}},\,\underline{\underline{D}},\,\underline{\underline{K}},\,\underline{\underline{G}} \quad , \qquad \text{Eq. 10}$$

so that the equation of motion becomes

$$\underline{\underline{M}}_{red}\,\ddot{\underline{x}}_{\mathbb{M}} + \left(\underline{\underline{D}}_{red} + \Omega\underline{\underline{G}}_{red}\right)\dot{\underline{x}}_{\mathbb{M}} + \underline{\underline{K}}_{red}\underline{x}_{\mathbb{M}} \quad . \qquad \text{Eq. 11}$$

4 HYDRODYNAMIC - JOURNAL BEARINGS

Beside the mechanical model, also the nonlinear interaction of the bearings with the rotor has to be described to allow for realistic system behaviour even under dynamical conditions.

4.1 Online solution of Reynolds lubrication equation

Starting from conservation of mass and momentum for an infinitesimal volume element the Navier-Stokes equations can be formulated. Further, by taking into account geometrical dimensions and relations between velocities and fluid-flows in different direction in the lubricating gap the Reynolds lubrication equation can be derived

$$\frac{\partial}{\partial x_g}\left(\frac{\rho\,h^3}{12\eta}\frac{\partial p}{\partial x_g}\right) + \frac{\partial}{\partial z}\left(\frac{\rho\,h^3}{12\eta}\frac{\partial p}{\partial z}\right) = \frac{\Omega\,r_s}{2}\frac{\partial(\rho\,h)}{\partial x_g} + \frac{\partial(\rho\,h)}{\partial t} \quad , \qquad \text{Eq. 12}$$

where p denotes the hydrodynamic pressure, h the gap function, Ω the rotational speed and r_s the radius of the shaft. Finally ρ and η are the relevant material parameters density and dynamic viscosity of the oil (7).

The solution of this partial elliptical differential equation is possible in a closed form only for special cases of short and long bearings. Therefore a numerical method (FDM, FVM, FEM) has to be used to enable the transformation into a system of linear equations by discretisation of the equation in the solution area (8), (9).

By solving the system, negative pressure values appear formally, which can be transmitted by fluids only to a very limited extend. Physically, the lubrication gap diverges, on the one hand dissolved air in the fluid escapes and additional air is drawn in via the axial boundaries whereas on the other hand the fluid vaporizes (both phenomena are known as cavitation). Resulting, a two-phase flow of fluid and compressible gas occurs. For modelling of the cavitation behaviour and in order to achieve a physical correct solution, various methods differing in accuracy and necessary computing time (JFO-theory (10), Elrod-algorithm (11), (12)) exist. Despite this, with regard to the task of a dynamic simulation, the negative pressures are set to zero (Gümbel cavitation algorithm) (13).

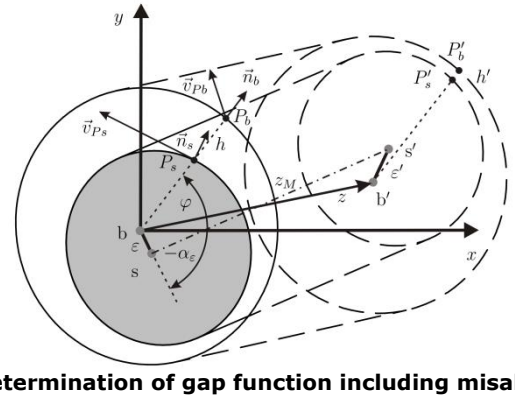

Figure 3 - Determination of gap function including misalignment

Usually, lookup tables for the bearing stiffness and damping properties based on the linearized Reynolds equation are used. The nonlinear behaviour is modelled exactly at the calculated states, deviations of these nominal states are determined by interpolation (14). Problems arise especially when in addition to the pure translational movement of the shaft also rotations around the transverse axes occur, e.g. due to unbalance response or bending of the shaft. Thus, the dimensionality of the lookup tables rises and therefore the organisational effort increases drastically. If these effects have a significant influence, the numerical solution of the Reynolds lubrication equation is inevitable.
With focus on the dynamic behaviour of the rotor, the formulation of the gap function h and its time derivation $\dot{h}$ in each journal bearing including misalignment is essential and can be accomplished as illustrated in Figure 3.
The gap function is derived by calculating the eccentricity $\varepsilon(z)$ in each axial position z of the bearing, which leads to

$$h = C - \varepsilon(z)\cos(\varphi - \alpha_\varepsilon(z)) \quad . \qquad \text{Eq. 13}$$

The first derivate of the gap function $\dot{h}$ has to be evaluated from the absolute velocities of the shaft- and the housing surface, which are functions of the corresponding translational velocities $\underline{v}_{s/b}$ and the angular velocities $\underline{\omega}_{s/b}$. Under usage of the normal fractions v_{Pbn} and v_{Psn}

$$\begin{aligned} v_{Psn} &= \underline{v}_{Ps}(\underline{v}_s, \underline{\omega}_s) \cdot \underline{n}_s \\ v_{Pbn} &= \underline{v}_{Pb}(\underline{v}_b, \underline{\omega}_b) \cdot \underline{n}_b \end{aligned} \qquad \text{Eq. 14}$$

$\dot{h}$ can be formulated by

$$\dot{h} = v_{Pbn} - v_{Psn} \quad . \qquad \text{Eq. 15}$$

4.2 Scheme for holistic simulation

For the holistic simulation by means of a direct interaction between the mechanical system and the hydrodynamic field problem of the journal bearings, an implementation of the nonlinear force laws in the dynamic simulation has to be realised (15).

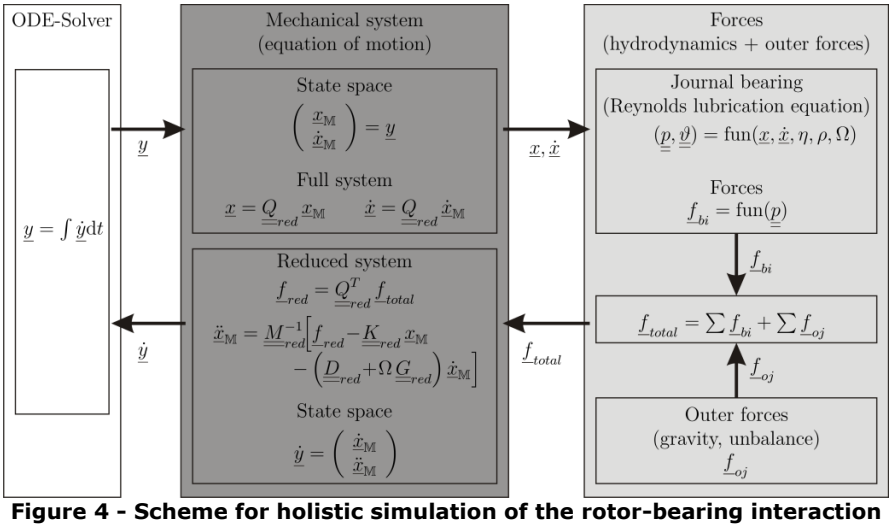

Figure 4 - Scheme for holistic simulation of the rotor-bearing interaction

The top level instance is the time integration which solves the rotor system's equation of motion in the state space. In every time step of the solver (including calculation of the jacobian etc.) the mechanical states are used to calculate the necessary input quantities (gap-function and its time derivative) for the online solution of the Reynolds lubrication equation. The resulting pressure is integrated to acting forces and moments, which represents the nonlinear behaviour of the bearings. Together with the outer forces due to gravity and unbalance the force vector can be evaluated. As result of the acting forces the accelerations of the overall system can be calculated and integrated in state space leading to the next time step (see Figure 4).

4.3 Modelling depth

For the further investigation three different modelling approaches V1-V3 are introduced.

V1 full approach: The general implementation of the solution of the Reynolds differential equation - as described in chapter 4.1 - in the time integration allows a detailed study of the dynamic system behaviour and the influence of individual parameters.

V2 look-up-table analogy:

Specifically, the misalignment in the bearings is neglected in the majority of studies and simulation methods or is predefined by a value based on linear estimations. These simplifications are in good agreement with those of popular solution using lookup tables (16); hence this variant is of particular importance. In order to investigate the influence of these assumptions a force element was adapted, which ignores the misalignment $\partial h/\partial z = 0,\ \partial \dot{h}/\partial z = 0$ (see Figure 3) and solves the Reynolds differential equation on the basis of displacement and velocity of the bearing center.

V3 short bearing approximation:

Assuming that the bearing width is much smaller than the circumference (short bearing) the Reynolds equation can be written as

$$\frac{\partial}{\partial z}\left(\frac{\rho\, h^3}{12\eta}\frac{\partial p}{\partial z}\right) = \frac{\Omega\, r_s}{2}\frac{\partial(\rho\, h)}{\partial x_g} + \frac{\partial(\rho\, h)}{\partial t} \quad . \qquad \text{Eq. 16}$$

If further the misalignment can be neglected and the material parameters of the fluid in the lubricating gap are constant $\rho,\ \eta \neq \mathrm{fun}(x_g, z)$, the variables can be separated formally and the pressure distribution can be determined analytically

$$p(z) = \frac{12\eta}{h^3}\left(\frac{\Omega\, r_s}{2}\frac{\partial h}{\partial x_g} + \frac{\partial h}{\partial t}\right)\frac{z^2}{2} - \frac{b^2}{8} + p_{amb} \quad , \qquad \text{Eq. 17}$$

where p_{amb} denote the ambient pressure. To minimize the numerical effort this form is often preferred for dynamic analyses, although the results in the context of the defined assumptions have to be scrutinized.

5 RESULTS

To analyse the dynamic system behaviour, at first steady-state conditions are modelled with a nominal unbalance. To assure that all initial disturbances are vanished, the system is simulated until at $t = 1\,s$ the unbalance suddenly increases to model the blade fracture. As a result, the acting forces increase drastically as well as the bearing forces and the vibration amplitudes. Figure 5 shows a scaled deformation of the turbine train after the blade failure.

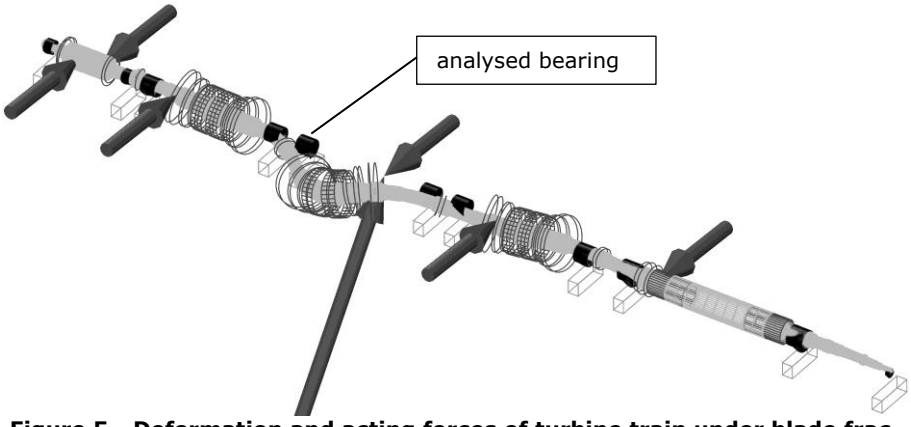

Figure 5 - Deformation and acting forces of turbine train under blade fracture conditions

To determine the influence of the varying modelling depth for the journal bearings, the essential output quantities are compared.

5.1 Steady state: unbalance response

Figure 7 shows the minimal gap in the analysed bearing. In the steady state region until $t = 1\,s$ the minimal gap has a dominant constant part $h_{min,mean} \approx 100\mu m$ due to the gravity force, which is superposed by small vibrations $h_{min,harm} \approx 5\mu m$ as result of the unbalance. The mean value differs only slightly by $h_{min,V1-V2} \approx 15\mu m$ between the version with and without misalignment (which occurs due to unbalance and bending), whereas the short bearing theory shows larger differences with respect to the full model $h_{min,V1-V3} \approx 30\mu m$. As a result of the medium loading (Sommerfeldnumber $So = \frac{\bar{F}\,\psi^2}{b\,d\,\eta\,\omega} = 4.3$) the bearing forces in Figure 6 show comparable values $f_{bearing} \approx 1.8 \cdot 10^6 N$ in the steady state region.

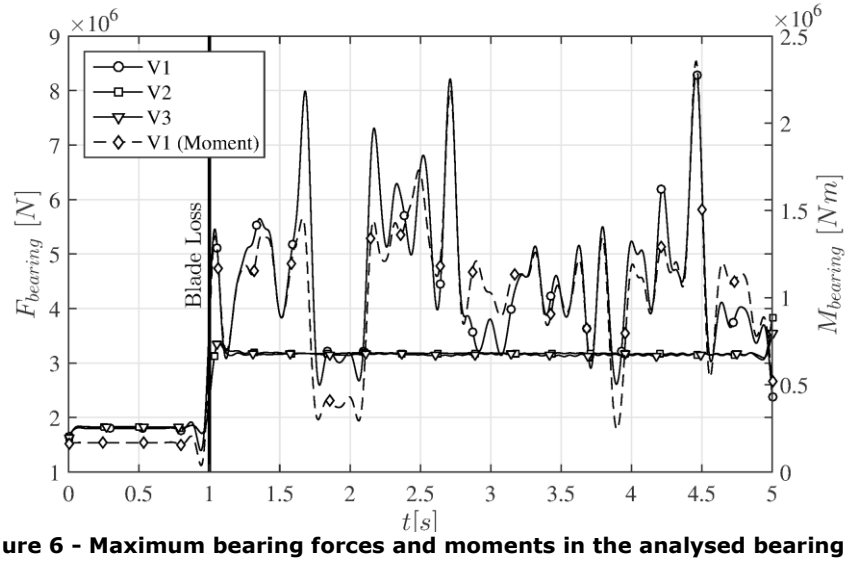

Figure 6 - Maximum bearing forces and moments in the analysed bearing depending on time

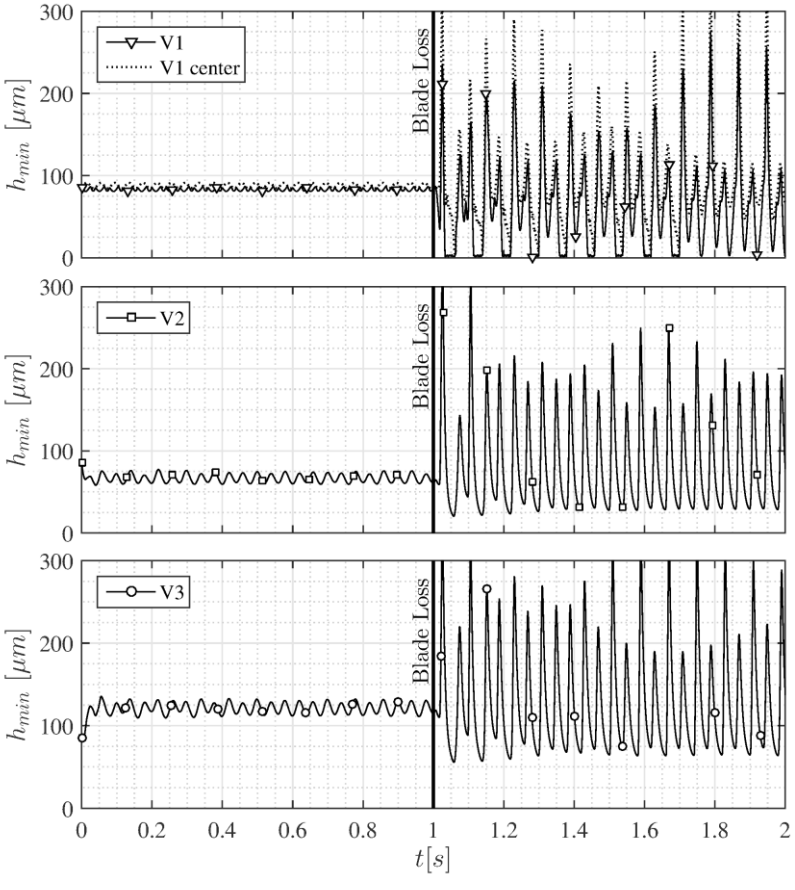

Figure 7 - Minimal gap in the analysed bearing (top: full Reynolds with misalignment, center: full Reynolds without misalignment, bottom: short bearing theory)

Beside the hydrodynamic quantities, also the maximum vibration amplitudes presented in Figure 8 and the normal stresses in Figure 9 are relevant results for rotordynamic respectively structural dynamic analyses. Again there are some minor differences, but due to the moderate load and the steady state conditions the vibration amplitudes reach consistent values $x_{max} \approx 0.3mm$ and the normal stresses are similar for all modelling approaches $\sigma_{bmax} \approx 40N/mm^2$.

From the steady state point of view all variants for the description of the nonlinear behaviour of the system are suitable and there would be no need for an extended simulation method including the numerical solution of the Reynolds lubrication equation or the consideration of misalignment.

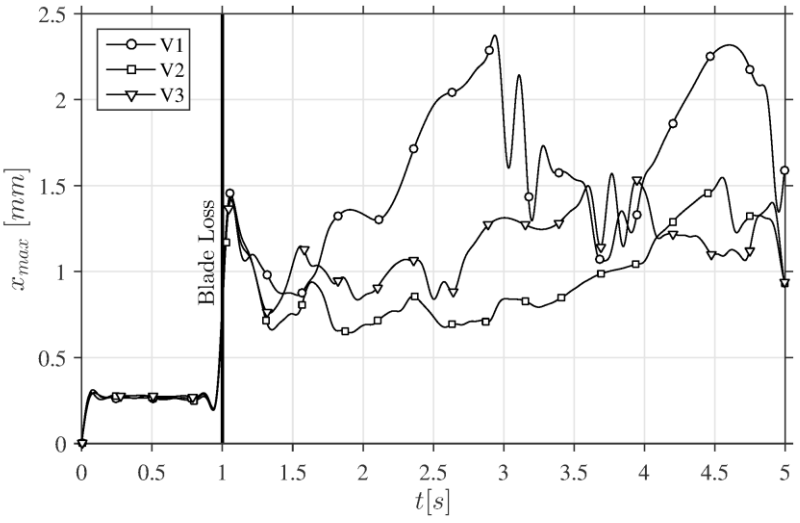

Figure 8 - Maximum vibration amplitudes in the shaft depending on time

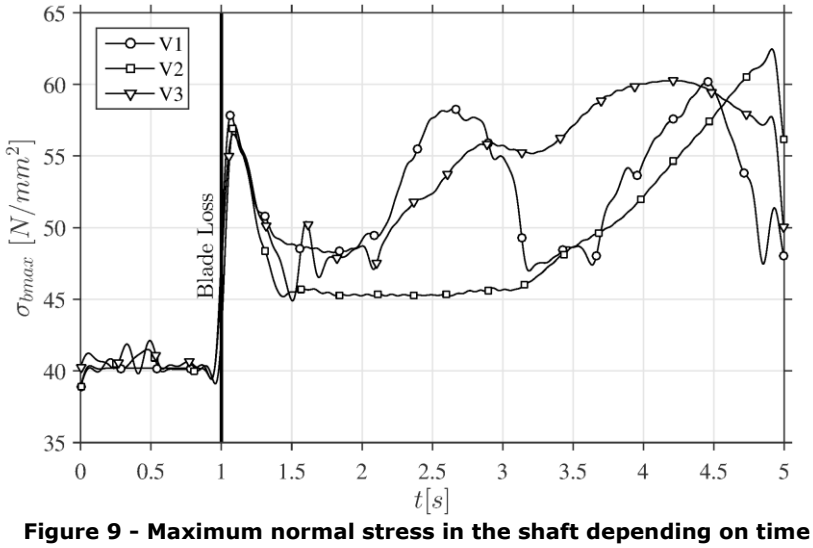

Figure 9 - Maximum normal stress in the shaft depending on time

5.2 Transient: abrupt blade failure

While in case of steady-state conditions the results for the bearing quantities are in good agreement, the transient analysis shows significant differences after the blade loss. Figure 7 shows, that the minimal gap after the blade fracture at $t = 1\,s$ has regions in which solid contact[1] occurs $h_{min} \approx 0\mu m$. Due to the misalignment, the minimal gap is not constantly at the same axial position - for sake of comparison additionally the centerline minimal gap is plotted.

[1] The contact is modelled using the Greenwood-Williamson-Tripp approach (17).

The model without misalignment is not able to show this behaviour, the lower minimal values and increased amplitudes here are a result of the higher unbalance compared to the steady-state case. The differences are obvious, while model V1 predicts a critical failure, the results of the approach V2 would be tolerable. This underlines the necessity to include misalignment in the description of the bearings. The differences to the short bearing theory are even bigger. The simulated behaviour seems to be uncritical and there would be no reason to shut down the turbine train, if only the approach V3 is available.
The high unbalance as a consequence of the blade loss causes the mean value of the bearing forces to increase drastically ($So = \frac{\bar{F}\,\psi^2}{b\,d\,\eta\,\omega} = 7.7$), Figure 6. Additionally, due to the highly dynamical changes of contact condition the bearing forces are fluctuating in the model V1 whereas the simplifications show an increased load level but only slight dynamical influences and by that underestimate the maximum forces by factor 3. Furthermore the bearing moments reaches significant values and should not be ignored.
Taking a look at the maximum vibration amplitudes and maximum normal stresses in Figure 8 and Figure 9 the differences as result of the bearing forces and the bearing moment, which is only present under consideration of misalignment, are obvious. By comparing these integral results the modelling depth leads to significant discrepancies even between the simplified approaches V2 and V3, although the trend is not clear (the maximum vibration amplitudes of V2 are lower than for the approach V3 but for the maximum normal stresses this behaviour switches).

6 CONCLUSION

The paper at hand described a holistic simulation method for rotordynamic problems including a detailed description of the journal bearings, which is necessary due to the significant influence on the system behaviour.
Especially for rotordynamic tasks and transient conditions the usual modelling depth of the bearings is generally rather low. The presented results show a significant influence of the bearing implementation upon tribological parameters and also rotordynamical quantities. For steady-state conditions the modelling depth leads to some minor differences, which after a sudden change of the unbalance resulting from an assumed blade failure increase drastically. Whereas the full model determines solid contact in some bearings, the simplified models show a uncritical bearing behaviour due to the neglected misalignment. As a result, the bearing forces are underestimated and the vibration and stresses are calculated to low pretending sufficient load capacities and a tolerable system behaviour.
Although the numerical effort for a holistic solution including a detailed description of the bearings with misalignment effects is rather high, the results especially for dynamical simulations and large displacements require such high modelling depth.

REFERENCE LIST

(1) H. D. Nelson (1980) *A finite rotating shaft element using timoshenko beam theory*. Journal of Mechanical Design, **102 (4),** 793–803
(2) O'Callahan, J. (1989) *System equivalent reduction and expansion process*. Proceedings of the 7th International Modal analysis conference, Society of Experimental Mechanics, **7**, 29 – 37
(3) Krenek, K. (2012) *Modellordnungsreduktion großer Systeme unter rotordynamischem Einfluss*. University Munich, Dissertation
(4) Guyan, R. J. (1965) *Reduction of Stiffness and Mass Matrices*. AIAA Journal, **3(2)**, 380
(5) Craig, R. R. J.; Bampton, M. C. C. (1968) *Coupling of Substructures for Dynamic Analysis*. AIAA Journal, **6(7)**, 1313 – 1319
(6) O'Callahan, J. (1989) *A procedure for an improved reduced system (IRS)*. Proceedings of the 7th International Modal analysis conference, Society of Experimental Mechanics, **7**, 17 – 21

(7) Pinkus, O.; Sternlicht, B. (1961) *Theory of hydrodynamic lubrication*. McGraw-Hill
(8) Booker, J. F.; Huebner, K. H. (1972) *Application of Finite Element Methods to Lubrication: An Engineering Approach*. Journal of Tribology, **84**, 323-323
(9) Vijayaraghavan, D.; Keith, T. G. (1989) *Development and Evaluation of a Cavitation Algorithm.* Tribology Transactions, **32**, 225-233
(10) Olsson, K. O. (1965) *Cavitation in dynamically loaded bearings*. Transactions of Chalmers University of Technology, **308**
(11) Elrod, H. G. (1981) *A Cavitation Algorithm*. Journal of Lubrication Technology, **103**, 350 – 354
(12) Nitzschke, S.; Woschke, E.; Schmicker, D.; Strackeljan, J. (2016) *Regularised cavitation algorithm for use in transient rotor dynamic analysis.* International Journal of Mechanical Sciences, **113**, 175–183
(13) Woschke, E.; Göbel, S.; Nitzschke, S.; Daniel, C.; Strackeljan, J. (2015) *Influence of bearing geometry of automotive turbochargers on the nonlinear vibrations during run-up*. Proceedings of the 9th IFToMM International Conference on Rotor Dynamics, Springer International Publishing, 835-844
(14) Lund, J. W. (1987) *Review of the Concept of Dynamic Coefficients for Fluid Film Journal Bearings*. Journal of Tribology, **109**, 37-41
(15) Daniel, C.; Strackeljan, J.; Woschke, E. (2008) *Enhanced fluid bearing simulation with standard multi body systems*, PAMM, **8**, 10111-10112
(16) Strackeljan, J.; Nitzschke, S.; Hagemann, T. (2012) *Use of ALP3T for journal bearing representation in MBS software Simpack.* FVA Nr. 622
(17) Kogut, L.; Etsion, I. (2002) *Elastic-Plastic Contact Analysis of a Sphere and a Rigid Flat.* Journal of Applied Mechanics, **69**, 657-662